JUNA Program PROPOSAL

Program 2: Direct measurement of the main s-process neutron source reaction, $^{13}C(a,n)^{16}O$, at stellar energies

1. Abstract

The $^{13}C(\alpha,n)^{16}O$ reaction is the key neutron source reaction for the main s-process nucleosynthesis. Due to the existence of sub-threshold resonances, there is a rather large uncertainty in this important reaction rate which limits our understanding to the nucleosynthesis of heavy elements. We will take the advantage of the ultralow background in Jinping underground lab, the first underground high current accelerator based on an ECR source and high sensitive neutron detector to study directly this important reaction for the first time within its relevant stellar energy range. Our result will be crucially important for testing and calibrating the predictive power of extrapolating model, providing a reliable astrophysical reaction rate, and eliminating one important uncertainty in stellar nucleosynthesis model.

2. Physics background

The origin of elements heavier than iron is one of the 11 greatest unanswered questions of physics for our 21st century [1]. By now, we believed that about 50% of the elements heavier than iron in our solar system are produced by the slow neutron capture process (s-process) while another about 50% of them are coming from the rapid neutron capture process (r-process). Both modern theory and observation have indicated that the main s-process happens in AGB stars.

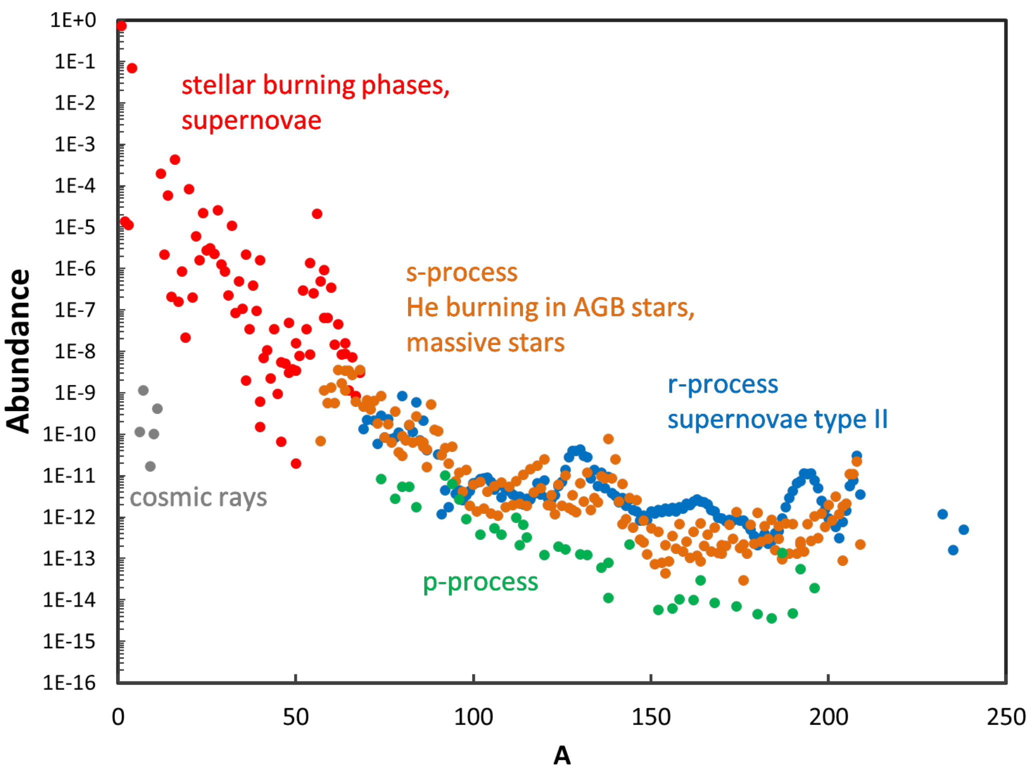

Fig. 1 The solar abundances and the corresponding nucleosynthetic processes.

R-process is a complicated and not well understood process involving many unknown neutron-rich isotopes. And we do not know the exact sites at which the r-process happens. The current solar r-process abundance is obtained by subtracting the contribution of s-process from the total solar abundance. The uncertainty of the s-process model affects our understanding to the solar r-process pattern. Therefore, a precise understanding of the s-process nucleosynthesis is essential to the study of the r-process nucleosynthesis.

The effective energy range (Gamow window) for the $^{13}C(\alpha,n)^{16}O$ reaction during the s-process spans from 140 to 230 keV in the center of mass frame. The excitation function and the corresponding s-factor are shown in Fig. 3. Because of the Coulomb barrier, the cross sections drop exponentially. e. g. the cross section is only about 10^{-14} b at the middle of Gamow window, E_{cm}=190 keV.

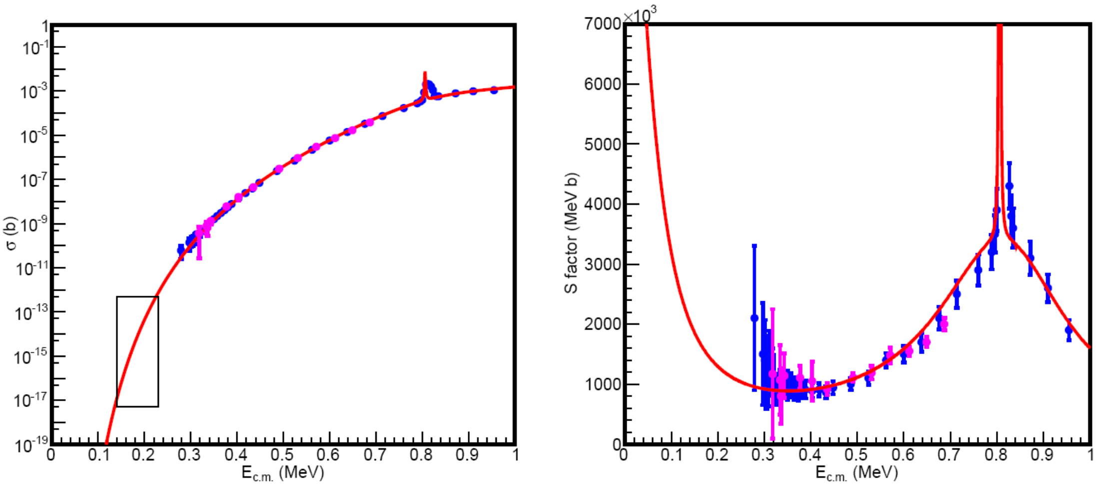

Fig. 2 (Left) The excitation function for the $^{13}C(\alpha,n)^{16}O$ reaction. The rectangle represents the important stellar energy range and the corresponding cross section. (Right) Astrophysical s-factor for the $^{13}C(\alpha,n)^{16}O$ reaction. The purple and blue points are the data from Ref. [2,7]. Due to the subthreshold resonance at E_{cm}=-3 keV (E_x=6.356 MeV), the extrapolated s-factor increases rapidly within the stellar energy range.

In the past half a century, a number of measurements have been performed in ground based laboratories to measure directly the $^{13}C(\alpha,n)^{16}O$ cross sections at low energies. These experiments are summarized in Table 1. In these experiments, two major difficulties limit the minimum measurable cross section and prevent our reach to the stellar energies. The first limitation is the background incurred by cosmic rays. In the Stuttgart experiment, which holds the world record of measuring the lowest $^{13}C(\alpha,n)^{16}O$ cross section, the neutron background in their detection system is about 7000 events/day. The other limitation is that beam current limits the reaction yield at an unmeasurable level. The minimum measured cross section is about 2 to 6 orders of magnitudes higher than the cross sections at stellar energies. To obtain these cross sections at lower energies, we have to rely on the R-matrix extrapolation based on the measured data at high energies. At stellar energies, the major contribution is dominated by a board sub-threshold resonance locating at E_{cm}=-3 keV (E_x=6.356 MeV, $J^{\pi}=1/2^+$). Besides that, another two subthreshold resonances with E_{cm}=-420 keV and -490 keV are suspected to play some role as well. The present direct measurement has only reached E_{cm}=0.279 MeV at which the error of the measured cross section is more than 60%. Because of their large errorbars and not being sensitive to the important subthreshold resonances, these poorly measured low energy data cannot place a strong constrain on the lower energy extrapolation. To provide better constrain on the subthreshold, two indirect methods, alpha cluster transfer reaction and Trojan horse method, have been introduced in the R-matrix extrapolation. While the statistical uncertainty of extrapolated cross sections is reduced, the statistical error associated with the indirect method remains unknown.

Table 1，Summary of the direct measurement of the $^{13}C(\alpha,n)^{16}O$ reaction

Reference	E_{cm}（MeV）	minimum measured cross section（b）	Year
Sekharan [3]	1.53—5.57	$(1.70\pm0.87)\times10^{-2}$	1967
Bair and Haas [4]	0.765---4.14	$(2.10\pm0.42)\times10^{-5}$	1973
Davids [5]	0.36—0.54	$(2.90\pm0.29)\times10^{-9}$	1968
Brune and Kellogg [6]	0.343-0.799	$(8.94\pm1.79)\times10^{-10}$	1993
Heil [2]	0.318-0.687	$(3.7\pm3.5)\times10^{-10}$	2008
Drotleff [7]	0.279-1.062	$(6.1\pm3.7)\times10^{-11}$	1993

The recommended $^{13}C(\alpha,n)^{16}O$ reaction rate at T_9=0.1 is summarized in Ref. [12]. The difference between highest limit and lowest limit is about a factor of 8. This large uncertainty affects our understanding to the s-process nucleosynthesis. Guo and Lugaro have investigated how the different $^{13}C(\alpha,n)^{16}O$ rates, recommended by CF88, NACER and the their rate, impact the s-process yield for some key isotopes [12]. Result from one of their model is shown in Fig. ?. To obtain a s-process yield with an error better than 5%, we need to constrain the $^{13}C(\alpha,n)^{16}O$ reaction rate uncertainty in a range of 20% or better.

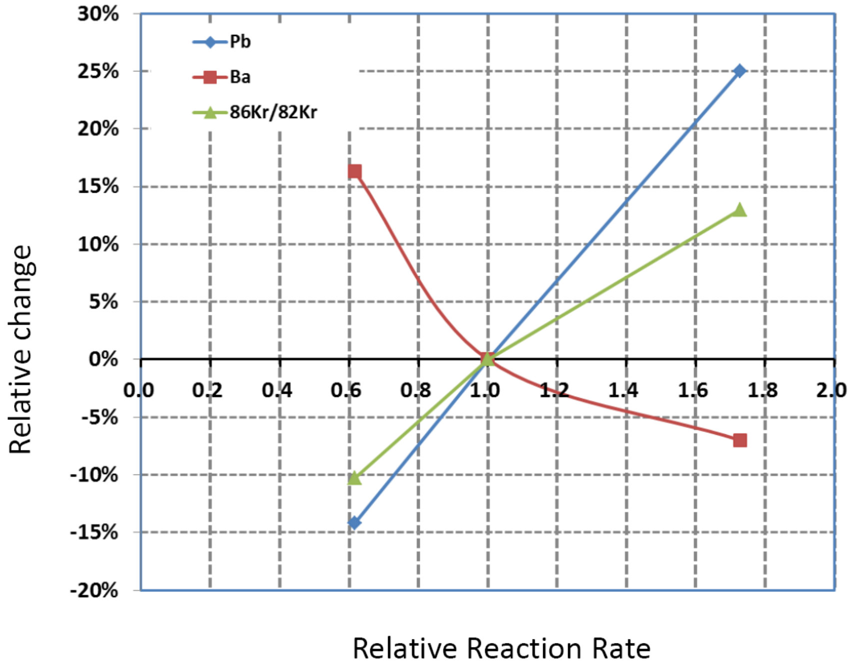

Fig. 3 The impacts of three different $^{13}C(\alpha,n)^{16}O$ reaction rates (CF88, CIAE and NACRE) to the production yield of the s-process in AGB stellar model. The x-axis is the relative 13C(a,n)16O reaction rates normalized by the CIAE rate. After normalization, the CF88 and NACRE rates are about 0.6 and 1.7, respectively. The y-axis represents the relative change of the stellar yield predicted by the AGB stellar model. The original data is taken from Ref. [11].

The most unambiguous way to determine the $^{13}C(\alpha,n)^{16}O$ rate is to directly measure the cross section right at the stellar energies. At least, the direct measurement should be carried out within the energy range at which the subthreshold resonance plays the dominant role. By this way, the theoretical systematic error can be reduced to its minimum. Therefore, it is essential to improve the experimental sensitivity so that we may push the measurement closer to or right at the stellar energies.

For the experimental study of reactions with ultra-low yields, the figure of merit (FOM) [16] can be defined as

$$F.O.M. = \frac{\text{Signal rate}}{\sqrt{\text{Background rate}}}$$

Therefore, the keys of studying the $^{13}C(\alpha,n)^{16}O$ reaction at lower energies are:

1) Increasing the beam intensity to achieve measurable yield
2) Decreasing the experimental background.

The current project is one of the four physics programs of the major research project, “The underground experimental study of the key problems in nuclear astrophysics”, supported by NSFC. The goal is to take the advantage of the ultralow background in Jinping underground lab, the first underground high current accelerator based on an ECR source and high sensitive neutron detector to study directly the $^{13}C(\alpha,n)^{16}O$ reaction for the first time within its relevant stellar energy range. Our high current accelerator driven by a powerful ECR source will be the first of its kind in underground laboratories and provide 10 mA He^+ in the energy range of 50—400 keV. With the high current beam, ultralow natural background and highly sensitive fast neutron detector, we shall be able to extend our measurement down to E_{cm}=0.2 MeV, the middle of the Gamow window. Our result will be crucially important for testing and calibrating the predictive power of extrapolating model, providing a reliable astrophysical reaction rate, and eliminating one important uncertainty in AGB stellar model.

3. Scientific program

3.1 The ultralow neutron background environment

The neutron background in a deep underground lab is dominated by the neutrons coming from two sources: the fission of U/Th impurities in the surround environments and the alpha particle emitted by unstable isotopes reacting with the ^{13}C and ^{17}O through the (α,n) reaction. Detailed simulation estimates the neutron flux density in Jinping lab as 0.153×10^{-6} n/(cm^2*s), which is one of best neutron background among the underground lab [17]. To reduce the background, Tsinghua group has developed a heavy shielding composed of polyethene, lead, boron loaded polyethene, oxygen free copper and so on. According a Geant4 simulation shows that the neutron background within the 10 m^3 space right in the middle of shielding reaches 9 neutrons/day [19], which is about 3 orders of magnitude lower than the Stuttgart experiment (~7000 neutrons/day).

3.2 The most intense 4He+ beam in deep underground lab

The to-be-installed Jinping underground accelerator is the first underground high current accelerator driven by a powerful ECR source. It is designed to provide p, He^+, He^{2+}. The covered energy range is from 50 to 400 keV for He+. The maximum energy can be double if He^{2+} is used. The 2.45 GHz ECR source can provide more than 10 mA of He^+ which is a factor of 20 higher than the one achieved at LUNA.

3.3 The low background highly sensitive fast neutron detector

We are designing a fast neutron detector consisting of 24 3He proportional counters and a liquid scintillator. The schematic drawing of the detector is shown in Fig. 4. The scintillator has a cylindrical shape with a length of 0.4 m and a diameter of 0.4 m. The 24 ^3He counters are distributed in the two circles with radii of 0.1 m and 0.15 m, respectively.

The energies of neutrons from the $^{13}C(\alpha,n)^{16}O$ reaction are in the range of 2 to 3 MeV. The produced neutrons are firstly slowed down by the liquid scintillator. After their thermalization, some neutrons enter ^3He counters and are detected. With the coincidence between the fast signal from fast neutron slowing down inside the liquid scintillator and the delayed signal from the thermalized neutrons captured by the ^3He counters, we can effectively suppress the backgrounds in liquid scintillator and ^3He detectors. The detection efficiency after coincidence is above 20% for neutrons from the $^{13}C(\alpha,n)^{16}O$ reaction.

However, the coincidence cannot easily remove the correlated background. For example, in the decay chain of U/Th impurities in the stainless steel walls of ^3He counters, there is a possibility that some product emits beta particle and then alpha decay. If the alpha particle enters the liquid scintillator while the beta triggers the liquid scintillator, a correlated event will be recorded. To suppress this kind of background, we plan to analyze the waveforms from 3He counters to select the neutron events and reject alpha events [26]. As a tradeoff, the efficiency of the 3He counters will be decreased by 1/2. Therefore, the detection efficiency with coincidence between the ^{3}He counters and the liquid scintillator drops to 10%.

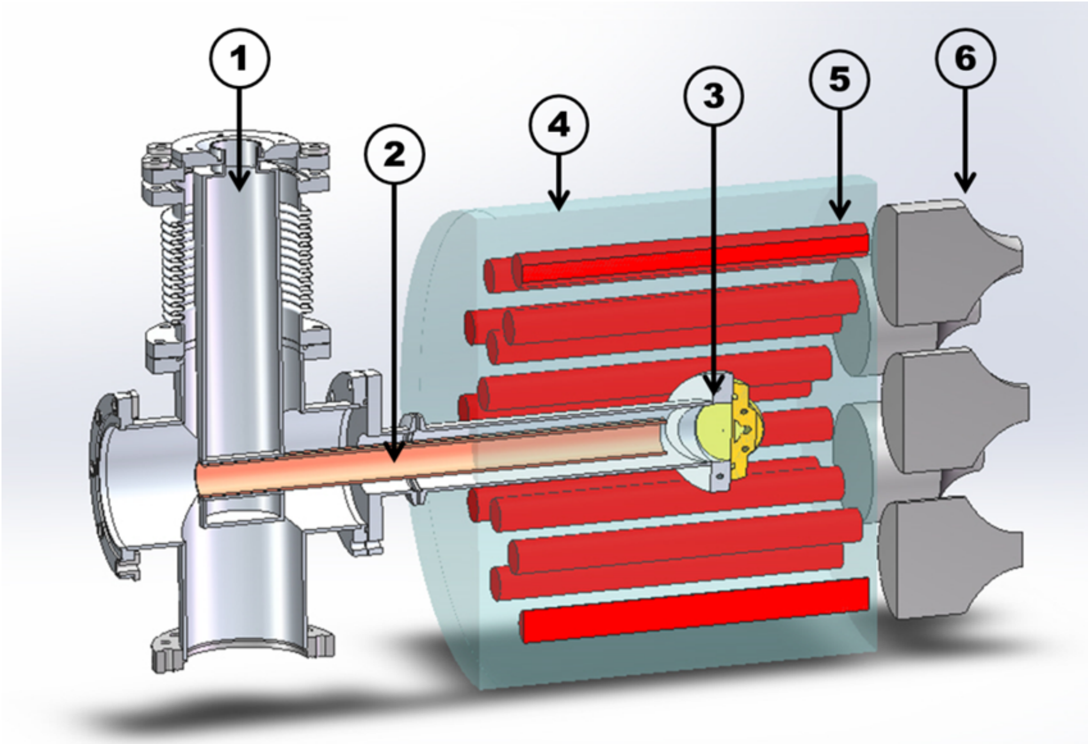

Fig. 4 Schematic drawing of low background highly sensitive fast neutron detector. 1) LN_2 cold trap; 2) Copper tube; 3) high power ^{13}C target; 4) Liquid scintillator; 5) ^{3}He detectors; 6) PMTs. The neutron shielding is not shown in this figure.

3.4 The natural and beam induced backgrounds

The natural background contribution in our detector comes from the detector material and the shielding material. As we discussed earlier, the neutron background in the 10 m^3 experimental space inside of the shielding is about 10 neutron/day. Assuming 1 ppb U/Th impurity in the stainless steel container, the fission neutron is about 0.05 neutrons/day. Therefore, the natural background is dominated by the U/Th impurity in the shieling material. Considering the 10% detection efficiency, the background rate is our detector is estimated as 1 event/day.

The beam included background can be induced by the He$^+$ beam reacting with the low-Z impurity inside of target and surrounding material. The cross section of ^{9}Be(α,n)^{12}C is about 6 orders of magnitude higher than the that of ^{13}C(α,n)^{16}O reaction. To minimize the low-Z impurity in target, we are planning to use implantation ^{13}C target and plate the inner surface of the beam tube with gold to prevent the He$^+$ beam reacting with the low-Z impurity in stainless steel. The D_2^+ is a potential contaminant in ^{4}He$^+$ beam due to their nearly identical mass to charge ratios. Another neutron background can be produced by the reactions, such as d(d,n)^{3}He and ^{6,7}Li(d,n). We are in the process of measuring the deuterium impurity in the beam out of an ECR source.

3.5 Estimation of reaction yield at E_{cm}=0.2 MeV

We plan to cover the energy range of E_{cm}=0.3 to 0.19 MeV with 120 days of beam time. In our experiment, thick target will be used instead of the traditional thin target to tolerate high beam power. We will measure the excitation function with thick target. The final cross section will be obtained by differentiation method [27].

Assuming a $^{4}He^{+}$ beam intensity of 10 mA, experimental period of 8 days and a detection efficiency of 10%, we expect to detect 58 events from the $^{13}C(\alpha,n)^{16}O$ reaction. The natural background events are 8 events according to the discussion in section 3.4. After subtracting the background, we can obtain the yield with a statistical error of 20%. Since LUNA accelerator can only provide 0.5 emA ^{4}He beam, they would need 1.4 years to achieve the same result, given that same background condition and same detection system.

This rough estimation does not include the beam induced background since we are lacking of the information of beam contaminant and low-Z impurity in our targets. We will need to re-evaluate the yield latter.

4. Work package and schedule

We divided our project into 5 sub-projects.

1) Neutron background estimation and measurement. A Gd loaded liquid scintillator has been developed to measure the fast neutron yield in Jinping underground lab. ^{3}He digitization is being carried out to improve its sensitivity to neutron event. By collaborating with Tsinghua, we will send these detectors to underground to measure the neutron background. The background data are expected to be available by the end of June, 2015.

2) Development of neutron detector. It includes detector design, development of prototype, and development of digital DAQ. The design of detection system will be finished by the end of June, 2015. The first prototype will be ready by the end of 2015. The ground based beam test and underground test will be finished by July, 2016.

3) High power ^{13}C target. It includes preparation of target, target nucleus profile and analysis of impurity, high power beam test, and beam current measurement. This work will be done in collaboration with the $^{12}C(\alpha,\gamma)^{16}O$ project. We expect it will be ready by the end of 2015.

4) Development of target station. It includes material impurity analysis, simulation of neutron background, design of neutron shielding and construction of target station. We expect it will be finished by July, 2016.

5) Beam energy calibration. It includes preparation of target, set up experimental station and test run using the existing 320 kV platform at IMP. This work will be finished by April, 2015.

5. Workforce

Name	Institute	Rank	Assignment
Xiaodong Tang	Institute of Modern Physics, CAS	Professor	Project manager
Xichao Ruan	China Institute of Atomic Energy	Professor	Liquid scintillator detector
Hanxiong Huang	China Institute of Atomic Energy	Associate Professor	Experimental design and electronics.
Xiongjun Chen	China Institute of Atomic Energy	Associate	Simulation and DAQ

		Professor	
Liyang Jiang	China Institute of Atomic Energy	Associate Professor	Target station and data analysis
Ningtao Zhang	Institute of Modern Physics, CAS	Associate Professor	Simulation and experimental design
Shuo Wang	Shandong University at Weihai	Assistant Professor	Target material analysis and simulation
Kuoang Li	China Institute of Atomic Energy	Assistant Professor	Beam energy calibration
Jie Ren	China Institute of Atomic Energy	Ph.D. Candidate	^{3}He detector waveform analysis and simulation
Zhijun Chen	Institute of Modern Physics, CAS	Master student	Data analysis
Tao Li	Institute of Modern Physics, CAS	Master student	High power target design
Han Chen	Institute of Modern Physics, CAS	Ph.D. Student	Development of detection system
Wanpeng Tan	University of Notre Dame	Associate Professor	Consultant
Maria Lugaro	Konkoly Observatory of the Hungarian Academy of Sciences	Scientist	Stellar evolution

6. Bibliography

[1] "Connecting Quarks with the Cosmos, Eleven Science Questoins for the New Century," Committee on the Physics of the Universe, Board on Physics and Astronomy, Division on Engineering and Physical Sciences, National Research Council of the National Academies, (2003).

[2] M.Heil et al., Phys. Rev. C78, 025803 (2008).

[3] K.K. Sekhara, et al., Phys. Rev. 156, 1187 (1967).

[4] J. K. Bair and F. X. Haas, Phys. Rev. C7, 1356 (1973).

[5] C. N. Davids, Nucl. Phys. A110, 619 (1968).

[6] C. R. Brune, I. Licot, and R. W. Kavanagh, Phys. Rev. C48, 3119 (1993).

[7] H. W. Drotleff, A. Denker, H. Knee, M. Soine, G. Wolf, J. W. Hammer, U. Greife, C. Rolfs, and H.P. Trautvetter, Astrophys. J.414, 735 (1993).

[8] S. Kubono et al., Phys. Rev. Lett. 90, 062501 (2003).

[9] E. D. Johnson et al., Phys. Rev. Lett. 97, 192701 (2006).

[10] M.G.Pellegriti et al., Phys.Rev. C 77, 042801 (2008).

[11] B. Guo et al., The Astrophysical Journal, 756:193 (2012).

[12] M. La Cognata et al., Phys.Rev.Lett. 109, 232701 (2012).

[13] G.Caughlan and W. Fowler, At. Data Nucl. Data Tables, 40, 283, (1988).

[14] Angulo, C., Arnould, M., Rayet, M., et al., Nucl. Phys. A, 656, 3 (1999).

[15] F. Käppeler, R. Gallino, S. Bisterzo, and Wako Aoki， Rev. Mod. Phys. 83, 157 (2011).

[16] J. M. Cesaratto et al., Nucl. Instr. and Meth. in Phys. Res. A623,888 (2010).

[17] S. Eichblatt, CDMS 97-01-25 (1997).

[18] Jie Ren, Master thesis, China Institute of Atomic Energy (2012).

[19] K. Kang et al., arXiv: ins-det/1303.0601v1, (2013).

[20] J. N. Abdurashitov et al., arXiv:nucl-exp/0607024v1, (2006).

[21] H. S. Lee et al., arXiv:astro-ph/0509080 (2005)

[22] V. Chazal et al., Astroparticle Physics 9, 163 (1998).

[23] F. Arneodo et al.,NUOVO CIMENTO A 8, 819-831 (1999).

[24] J. N. Abdurashitov et al., Particles and Nuclei, Letters, No. 6, 109 (2001)

[25] V. Tomasello, M. Robinson, and V.A. Kudryavtsev, Astroparticle Physics 34, 70 (2010)

[26] Langford et al., Nucl. Instr. Meth. A 717, 51 (2013)

[27] Notani et al., Phys. Rev. C 85, 014607 (2012)